6. Stenstam BH, Pellettieri L, Sorteberg W, Rezaei A, Sköld K (2007) BNCT for recurrent intracranial meningeal tumours: case reports. Acta Neurol Scand 115:243–247
7. Levin VA, Bidaut L, Hou P, Kumar AJ, Wefel JS, Bekele BN, Grewal J, Prabhu S, Loghin M, Gilbert MR, Jackson EF (2011) Randomized double-blind placebo-controlled trial of bevacizumab therapy for radiation necrosis of the central nervous system. Int J Radiat Oncol Biol Phys 79:1487–1495
8. Miyatake S, Furuse M, Kawabata S, Maruyama T, Kumabe T, Kuroiwa T, Ono K (2013) Bevacizumab treatment of symptomatic pseudoprogression after boron neutron capture therapy for recurrent malignant gliomas. Report of 2 cases. Neuro Oncol 15:650–655
9. Lou E, Sumrall AL, Turner S, Peters KB, Desjardins A, Vredenburgh JJ, McLendon RE, Herndon JEn, McSherry F, Norfleet J, Friedman HS, Reardon DA (2012) Bevacizumab therapy for adults with recurrent/progressive meningioma: a retrospective series. J Neurooncol 109:63–70
10. Nayak L, Iwamoto FM, Rudnick JD, Norden AD, Lee EQ, Drappatz J, Omuro A, Kaley TJ (2012) Atypical and anaplastic meningiomas treated with bevacizumab. J Neurooncol 109: 87–193
11. Puchner MJ, Hans VH, Harati A, Lohmann F, Glas M, Herrlinger U (2010) Bevacizumab-induced regression of anaplastic meningioma. Ann Oncol 21:2445–2446
12. Aziz T, Peress NS, Diaz A, Capala J, Chanana A (2000) Postmortem neuropathological features secondary to boron neutron capture therapy for glioblastoma multiforme. J Neuropathol Exp Neurol 59:62–73
13. Kageji T, Nagahiro S, Uyama S, Mizobuchi Y, Toi H, Nakamura M, Nakagawa Y (2004) Histopathological findings in autopsied glioblastoma patients treated by mixed neutron beam BNCT. J Neurooncol 68:25–32
14. Miyatake S, Kawabata S, Kajimoto Y, Aoki A, Yokoyama K, Yamada M, Kuroiwa T, Tsuji M, Imahori Y, Kirihata M, Sakurai Y, Masunaga S, Nagata K, Maruhashi A, Ono K (2005) Modified boron neutron capture therapy for malignant gliomas performed using epithermal neutron and two boron compounds with different accumulation mechanisms: an efficacy study based on findings on neuroimages. J Neurosurg 103:1000–1009
15. Miyatake S, Kawabata S, Nonoguchi N, Yokoyama K, Kuroiwa T, Matsui H, Ono K (2009) Pseudoprogression in boron neutron capture therapy for malignant gliomas and meningiomas. Neuro Oncol 11:430–436
16. Nakagawa N, Akai F, Fukawa N, Fujita Y, Suzuki M, Ono K, Taneda M (2007) Early effects of boron neutron capture therapy on rat glioma models. Brain Tumor Pathol 24:7–13
17. Sun T, Zhang Z, Li B, Chen G, Xie X, Wei Y, Wu J, Zhou Y, Du Z (2013) Boron neutron capture therapy induces cell cycle arrest and cell apoptosis of glioma stem/progenitor cells in vitro. Radiat Oncol 8:195
18. Wang P, Zhen H, Jiang X, Zhang W, Cheng X, Guo G, Mao X, Zhang X (2010) Boron neutron capture therapy induces apoptosis of glioma cells through Bcl-2/Bax. BMC Cancer 10:661

Practical Radiation Oncology (2015) 5, e9-e16

practical radiation oncology
pro
www.practicalradonc.org

Original Report

Long-term survival after treatment of glioblastoma multiforme with hyperfractionated concomitant boost proton beam therapy

Masashi Mizumoto PhD [a], Tetsuya Yamamoto PhD [b], Shingo Takano PhD [b], Eiichi Ishikawa PhD [b], Akira Matsumura PhD [b], Hitoshi Ishikawa PhD [a], Toshiyuki Okumura PhD [a], Hideyuki Sakurai PhD [a], Shin-Ichi Miyatake PhD [c], Koji Tsuboi PhD [a,b,*]

[a]*Proton Medical Research Center, University of Tsukuba, Tsukuba, Ibaraki, Japan*
[b]*Department of Neurosurgery, University of Tsukuba, Tsukuba, Ibaraki, Japan*
[c]*Department of Neurosurgery, Osaka Medical Collage, Osaka, Japan*

Received 1 December 2013; revised 24 March 2014; accepted 25 March 2014

Abstract

Purpose: Although conventional x-ray therapy of 60 Gy in 30 fractions is generally used in our institute as well as others, the prognosis of patients with glioblastoma multiforme (GBM) is poor. The purpose of this study was to evaluate the characteristics of long-term GBM survivors after postoperative hyperfractionated concomitant boost x-ray radiation therapy and proton beam therapy.

Methods and materials: Twenty-three of 81 GBM patients who met the eligible criteria and consented to the protocol were treated with x-ray radiation therapy (50.4 Gy in 28 fractions in T2-high areas) and proton beam therapy (46.2 GyE in 28 fractions in gadolinium-enhanced volumes >6 hours after x-ray radiation therapy) concurrent with nimustine hydrochloride or temozolomide.

Results: Treatment was completed in all patients within 38-50 days (median, 43 days). Six currently living patients (median follow-up period, 70.9 months) developed radiation necrosis without tumor recurrence. Of these, 5 underwent necrotomy and 2 received bevacizumab after necrotomy. Compared with the pretreatment status, the Karnofsky performance scale (KPS) for the 6 survivors decreased by 10%-30% at the last follow-up. However, radiation necrosis had been well controlled and 5 of 6 patients maintained a stable KPS without hospital care.

Conclusions: The results suggest that high-dose proton beam therapy could control GBM pathogenesis if the treatment area completely covers tumor infiltration. Although radiation necrosis was inevitable, the remaining brain volume was fairly well preserved in the long-term survivors.

Sources of support: This work was supported in part by Grants-in-Aid for Scientific Research (B) (24390286), Challenging Exploratory Research (24659556), Young Scientists (B) (25861064), and Scientific Research (C) (24591832) from the Ministry of Education, Science, Sports and Culture of Japan.
Conflicts of interest: None.

* Corresponding author. Proton Medical Research Center, Faculty of Medicine, University of Tsukuba, 1-1-1 Tennoudai, Tsukuba, Ibaraki, 305-8575 Japan.
E-mail address: tsuboi@pmrc.tsukuba.ac.jp (K. Tsuboi).

http://dx.doi.org/10.1016/j.prro.2014.03.012
1879-8500/

Introduction

The current standard of care for patients with glioblastoma multiforme (GBM) consists of maximum resection followed by 60 Gy of conventional x-ray radiation therapy concurrent with temozolomide administration.[1,2] Although a median survival period of 14.6 months has been achieved with this combination therapy, long-term survival rates are unsatisfactory, with a 2-year survival rate of only 26.5%.[2] Molecular targeted therapy[3,4] or immunotherapy in conjunction with conventional radiation therapy[5] with or without temozolomide was recently tested and found to have certain benefits in improving survival outcomes. Although these approaches are promising, their genuine clinical advantages require further investigation.

In radiation therapy, 60 Gy of x-rays in 30 fractions has been considered the maximum dose to avoid damage to normal brain tissue.[6] However, technologic advances in radiation therapy, such as proton beam therapy (PBT), intensity modulated radiation therapy, and stereotactic radiation therapy, have made it possible to deliver higher doses to the tumor while sparing healthy brain tissue.[7,8] This has led to the question of whether higher doses of radiation to the tumor can improve survival while maintaining quality of life for GBM patients. Several reports have suggested that high-dose radiation therapy can improve local control and survival in GBM patients.[7,8] Rusthoven et al[9] recently found that GBM patients with radiation necrosis at reoperation had improved survival compared with those without.

We previously reported that postoperative hyperfractionated concomitant boost PBT of 96.6 GyE in 56 fractions with nimustine hydrochloride was feasible and improved survival in GBM patients (median survival, 21.6 months).[10] We observed cases of long-term survivors without tumor recurrence during the follow-up of patients in this series and additional cases, and collected their serial magnetic resonance images over their entire clinical course. Thus, in this study we examined the characteristics of these long-term GBM survivors who underwent postoperative hyperfractionated concomitant boost PBT (96.6 GyE in 56 fractions).

Methods and materials

Patients

Between September 2001 and April 2009, 81 patients who were histologically diagnosed as GBM received postoperative radiation therapy at our institute. As our conventional standard radiation therapy we deliver 40 to 50 Gy in 20 to 25 fractions first to the area encompassing high intensity in T2-weighted MRI with a 2.0 cm margin. Subsequently, we add the remaining 10 to 20 Gy as a boost to the area encompassing contrast enhancement or the tumor bed plus a 2.0 cm margin, making a total dose of 60 Gy in 30 fractions. In some patients with poor general conditions such as Karnofsky performance scale (KPS) <40% or old age, consecutive daily treatment of 30 fractions is often difficult. In such cases, we reduce the total dose with smaller fraction numbers to shorten the treatment period. We usually deliver 45 Gy in 15 fractions to the contrast-enhanced area plus a 2 cm margin. Of these 81 patients, 58 received the aforementioned conventional radiation therapy; 41 were treated with doses from 60 to 61.2 Gy in 30 to 34 fractions, and 17 patients were treated with lower doses with smaller fraction numbers. The remaining 23 patients who met the eligible criteria[10,11] and consented on the basis of free will were prospectively enrolled in a phase 1/2 protocol for treatment with hyperfractionated concomitant boost PBT. A written informed consent based on each patient's will was obtained from all 23 patients (13 men, 10 women) prior to study enrollment. The patients had a median age of 56 years (range, 31-76 years). The KPS before PBT was 60% (n = 1), 70% (n = 5), 80% (n = 8), 90% (n = 7), and 100% (n = 2). Eight patients underwent partial resection and 15 underwent subtotal resection. The median MIB-1 labeling index was 29.6% (range, 3.8%-55.0%). The characteristics of the 23 patients are shown in Table 1.

Treatment methods

Treatment planning for PBT was performed using computed tomography images at 3-mm intervals in the treatment position. Proton beams were spread out and shaped with a ridge filter, double-scattering, multileaf collimators, and a custom-made bolus covering the target volume. All patients received hyperfractionated concomitant boost PBT after surgery.[10] The proton beam was generally delivered

Table 1 Characteristics of 23 patients

Characteristic	No.
Age (y)	31-76 (range) 56 (median)
Sex	
Male	13
Female	10
Karnofsky performance status	
60	1
70	5
80	8
90	7
100	2
Extent of surgery	
Partial resection	8
Subtotal resection	15
MIB-1 labeling index (%)	3.8-55.0 (range) 26.2 (median)

from 2 directions and all fields were treated daily. Clinical target volume 1 (CTV1) was defined as the area of contrast enhancement on magnetic resonance imaging (MRI) or the tumor bed, CTV2 was defined as CTV1 in addition to a 10-mm margin, and CTV3 was defined as the area surrounding edema determined by T2-weighted MRI or fluid-attenuated inversion recovery imaging. In the protocol, conventional x-ray radiation therapy or 250 MeV PBT (50.4 GyE in 28 fractions) was delivered to CTV3 in the morning. Concomitant boost PBT (23.1 GyE in 14 fractions) was delivered to CTV2 >6 hours after conventional radiation therapy, and subsequent PBT (23.1 GyE in 14 fractions) was delivered to CTV1. The planned target volume (PTV) was defined as CTV in addition to 5 mm for setup error. Total doses were 96.6 GyE in 56 fractions for PTV1, 73.5 GyE in 42 fractions for PTV2, and 50.4 Gy in 28 fractions for PTV3. The maximum dose was defined as 50 GyE to the optic chiasm and 60 GyE to the brain stem (dose to the entire brain stem was limited to 50 GyE).

Nimustine hydrochloride was administered intravenously at 80 mg/m^2 for 1 day in the first and fourth weeks of radiation therapy. Because concomitant chemotherapy was changed to temozolomide in August 2008, 2 patients were treated with hyperfractionated concomitant boost PBT concurrent with daily temozolomide (75 mg/m^2). Figure 1 shows a schematic diagram of our GBM treatment protocol.

Follow-up procedures and evaluation criteria

During treatment, acute treatment-related toxicities were assessed weekly in all patients. After completion of PBT, patients were evaluated by physical examination, MRI, and blood tests every 3 months for the first 2 years and every 6 months thereafter. The following 2 endpoints were evaluated: (1) MRI changes defined as development or enlargement of enhanced lesions on MRI to determine progression; and (2) death from any cause to estimate overall survival. The KPS was monitored before and after treatment and at the most recent follow-up. The Kaplan-Meier method was used to calculate MRI change-free and overall survival rates. Differences between groups were evaluated by the log-rank test. Acute and late treatment-related toxicities were assessed using the National Cancer Institute Common Terminology Criteria for Adverse Events, version 3.0, and the Radiation Therapy Oncology Group and European Organisation for Research and Treatment of Cancer (RTOG/EORTC) late radiation morbidity scoring scheme.[12] An in-field MRI change was defined as an event observed within CTV1 to which 96.6 GyE was delivered, a border MRI change was defined as an event within CTV2 or CTV3 to which 50.4-73.5 GyE was delivered, and an extra-field MRI change was defined as an event in the region outside CTV3.

Results

Background

All patients received x-ray radiation therapy and PBT within 3 months postoperatively. The period between surgery and initiation of radiation therapy was 15-87 days (median, 27 days), and x-ray radiation therapy and PBT

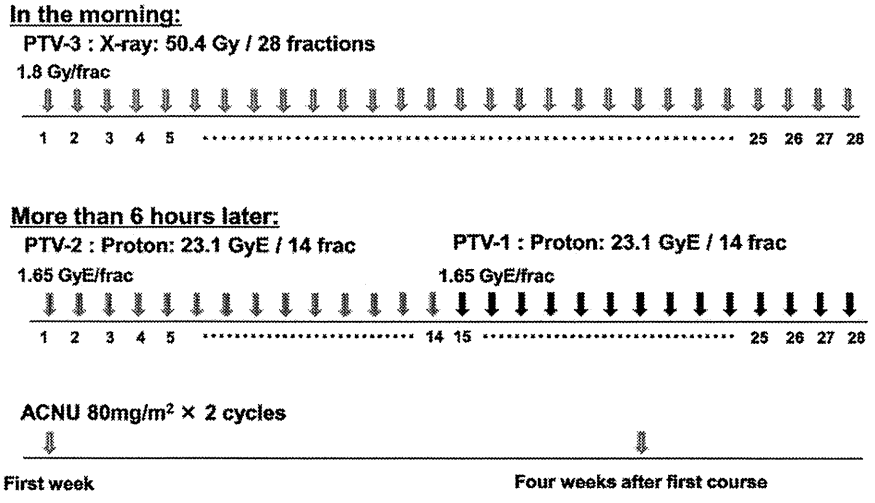

Figure 1 A schematic diagram of the treatment protocol for glioblastoma multiforme. Before August 2008, nimustine hydrochloride (ACNU) was administered intravenously at a dose of 80 mg/m^2 in the first and fourth weeks, thereafter, it was changed to concomitant daily use of temozolomide (75 mg/m^2). (PTV, planning target volume).

were administered over 38-50 days (median, 43 days). Of the 21 patients treated with nimustine hydrochloride, 17 received 2 cycles and 4 received 1 cycle. Of the 2 patients treated with temozolomide, 1 completed daily temozolomide concurrent with PBT and the other patient discontinued for 2 weeks because of neutropenia.

Toxicity

Grade 3 or higher acute hematologic toxicities occurred in 11 patients, probably due to nimustine hydrochloride.[10] Five patients with acute toxicity including nausea or headache were treated with corticosteroids during PBT. Grade 1 radiation dermatitis was observed in 2 patients and grade 2 was observed in 21 patients. In addition, all patients showed alopecia in the irradiated area. Late toxicity is discussed below.

Survival

The overall 1- and 2-year survival rates were 78% (95% CI, 61%-95%) and 43% (95% CI, 23%-63%), respectively, with a median survival period of 21.0 months (range, 5.5-81.0 months; 95% CI, 16.1-25.9 months; Fig 2). At the time of analysis, 6 patients were still alive with a median follow-up period of 70.9 months; all had survived >4 years after treatment. Fifteen patients died of tumor recurrence, and 2 died of unrelated diseases.

Magnetic resonance imaging changes

The 1- and 2-year MRI change-free survival rates of all 23 patients were 36% (95% CI, 16%-57%) and 13% (95% CI, 0%-28%), respectively (Fig 2). The median MRI change-free survival period was 9.0 months (range, 3.4-35.8 months; 95% CI, 7.0-10.9 months). the MRI changes defined as development or enlargement of enhanced lesion occurred in 20 patients, including 8 within CTV1 (96.6 GyE irradiation), 8 within CTV2 or CTV3 (≥50.4 GyE irradiation, but <96.6 GyE), and 4 outside the irradiated field. Six of the 8 patients with MRI changes within CTV1 had radiation necrosis without evidence of tumor recurrence. Five of these 6 patients were diagnosed by pathologic examination, and 1 patient was diagnosed by nuclear medicine study and MRI. All patients with MRI changes outside CTV1 were cases with tumor recurrence.

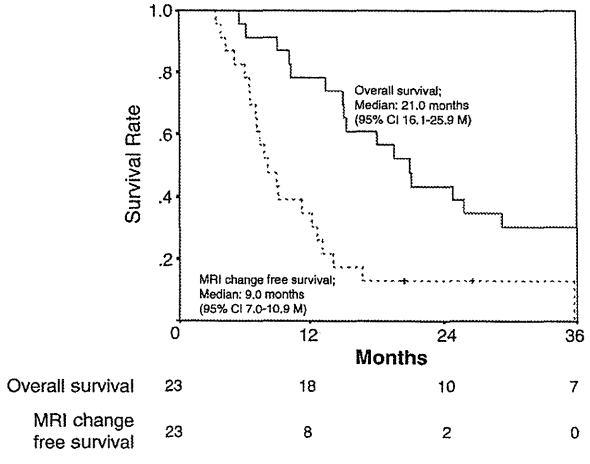

Figure 2 Kaplan-Meier estimates of overall survival and magnetic resonance imaging (MRI) change-free survival for all 23 patients. Tick marks indicate censored patients.

Long-term survivors

Upon follow-up of all 23 patients, 6 patients had radiation necrosis and 2 were diagnosed with leukoencephalopathy. The 6 patients with radiation necrosis survived at least 4 years after PBT without evidence of tumor recurrence. The median MRI change-free survival in patients with radiation necrosis was 12.7 months (range, 6.1-34.5 months; 95% CI, 6.6-18.8 months), whereas that of patients with GBM recurrence was 7.1 months (range, 3.4-12.6 months; 95% CI, 5.4-8.8 months; Fig 3). Two patients died at 19.5 and 25.8 months after radiation therapy without tumor recurrence on MRI. In these cases, marked cortical atrophy with diffuse white matter change was found on T2-weighted MRI, strongly indicating occurrence of leukoencephalopathy.

In survivors with radiation necrosis, KPS decreased by 10%-30% in the last follow-up compared with pretreatment KPS; however, 5 of the 6 patients maintained a stable KPS of >60%. The characteristics of the 6 survivors are shown in Table 2. The CTV1 in radiation necrosis cases was 13.4-46.2 cc (median, 20.6 cc) compared with 22.8-387.0 cc (median, 93.5 cc) in recurrent cases.

Case presentation (2 cases with or without bevacizumab treatment)

The typical clinical course for a long-term survivor with radiation necrosis is illustrated in Fig 4. Case 1 was a 46-year-old female with right temporal GBM (Fig 4A), and her pretreatment KPS was 90%. Following subtotal tumor resection, she received hyperfractionated concomitant boost PBT of 96.6 GyE in 56 fractions according to the protocol (Fig 4B,C). However, MRI changes appeared at the tumor bed 12 months after PBT, expanding slowly (Fig 4D,E). As neurologic symptoms progressed, a second surgery was performed 21 months after PBT (Fig 4F). The pathologic diagnosis at this time was radiation necrosis. In addition, because MRI showed that radiation necrosis had relapsed 42 months after PBT (Fig 4G), 6 courses of bevacizumab (5 mg/kg every 2 weeks) were performed.

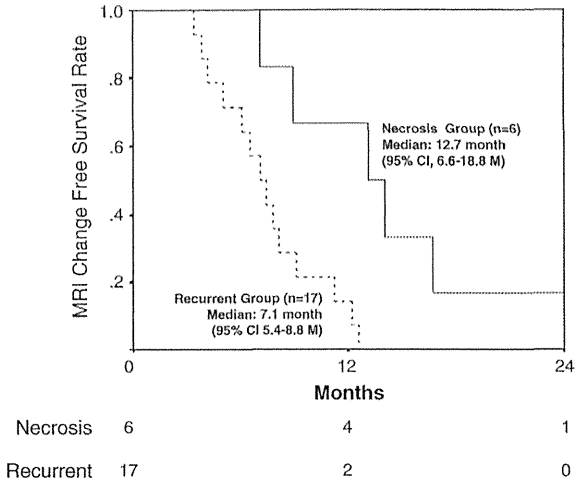

Figure 3 Kaplan-Meier estimates of magnetic resonance imaging (MRI) change-free survival for cases with radiation necrosis and recurrence. (CI, confidence interval.)

Following this therapy, radiation necrosis has been well controlled (Fig 4H) and her KPS maintained at 80%.

Case 2 was a 42-year-old woman with left temporal GBM (Fig 5A), and her pretreatment KPS was 100%. Following subtotal resection, she was treated with the same protocol as case 1 (Fig 5B,C). However, MRI changes appeared at the tumor bed 9 months after PBT (Fig 5D). Because tumor growth progressed gradually, the second surgery was performed 5 months later (Fig 5E), with a pathologic diagnosis of radiation necrosis. After the second resection, radiation necrosis remained stable for 40 months without further treatment (Fig 5F), and her KPS was maintained at 90%, manifesting slight sensory aphasia.

Discussion

Postoperative radiation therapy of 60 Gy in 30 fractions concurrent with temozolomide is the current standard of treatment for GBM patients. However, patient outcomes remain unsatisfactory.[1,2] Compared with conventional x-ray radiation therapy, the excellent dose concentricity of PBT allows delivery of higher doses to solid targets without residual damage to surrounding tissues,[13-19] possibly improving the prognosis of GBM patients. In a previous study,[10] we demonstrated that concomitant boost PBT of 96.6 GyE in 56 fractions improves patient survival with limited acute and late toxicity in GBM patients. Fitzeck et al[7] also found that a dose of 90 GyE with accelerated fractionation improved local GBM control and patient survival. In fact, exceptional control was achieved in the tissue area that received 90 GyE, whereas local recurrence was most frequently observed in areas that received $\leq$60-70 GyE. These results suggest that a PBT dose of $\geq$90 GyE may elicit effective control of GBM pathogenesis, in agreement with those of a study by McDonald et al,[11] which reported that >90% of failure patterns after conventional radiation therapy (60 Gy) plus temozolomide were central or in-field. Our study also demonstrated that 8 patients had MRI changes within the area irradiated with 96.6 GyE, and 6 of these patients were diagnosed with radiation necrosis without tumor recurrence. In contrast, the other 8 patients with MRI changes outside this area had only recurrence. Collectively, these results indicate that 96.6 GyE in 56 fractions can effectively control GBM growth, whereas $\leq$73.5 GyE is insufficient.

In our protocol, conventional x-ray radiation therapy or PBT (50.4 Gy in 28 fractions) was delivered to the T2-high area plus a 5-mm margin. Consequently, 4 patients showed recurrence at the marginal area in T2-weighted or fluid-attenuated inversion recovery MRI. This failure pattern may indicate an insufficient margination. Although we planned a 96.6 GyE distribution to the minimum essential area to avoid brain injury, a larger margination may be preferable, depending on tumor location and size, or additional diagnostic modalities, such as methionine positron emission computed tomography, should be applied to sufficiently cover the area of tumor invasion.

The median MRI change-free survival period (12.7 months) in the radiation necrosis group was approximately twice as long as that in the recurrent group. This indicates that radiation necrosis occurs later than tumor recurrence; thus, the incidence of radiation necrosis can be masked by tumor recurrence. Similarly, because conventional GBM treatment is associated with a low local control rate, the

Table 2 Clinical characteristics of 6 long-term survivors

No.	Age (y)	Sex	KPS before PBT (%)	CTV1 (cc)	Time to RN (mo)	Additional treatment for RN	Overall survival (mo)	Current KPS (%)
1	62	M	80	14.7	16.7	Surgery	76.8	60
2	49	F	90	46.2	7.1	Surgery	66.8	60
3	65	F	70	38.4	35.8	None	74.9	50
4	31	M	80	26.5	14.1	Surgery, bevacitumab	81.0	70
5	46	F	90	14.6	12.2	Surgery, bevacitumab	58.8	80
6	42	F	100	13.4	9.0	Surgery	52.8	90

CTV1, clinical target volume 1; KPS, Karnofsky performance status; PBT, proton beam therapy; RN, radiation necrosis.

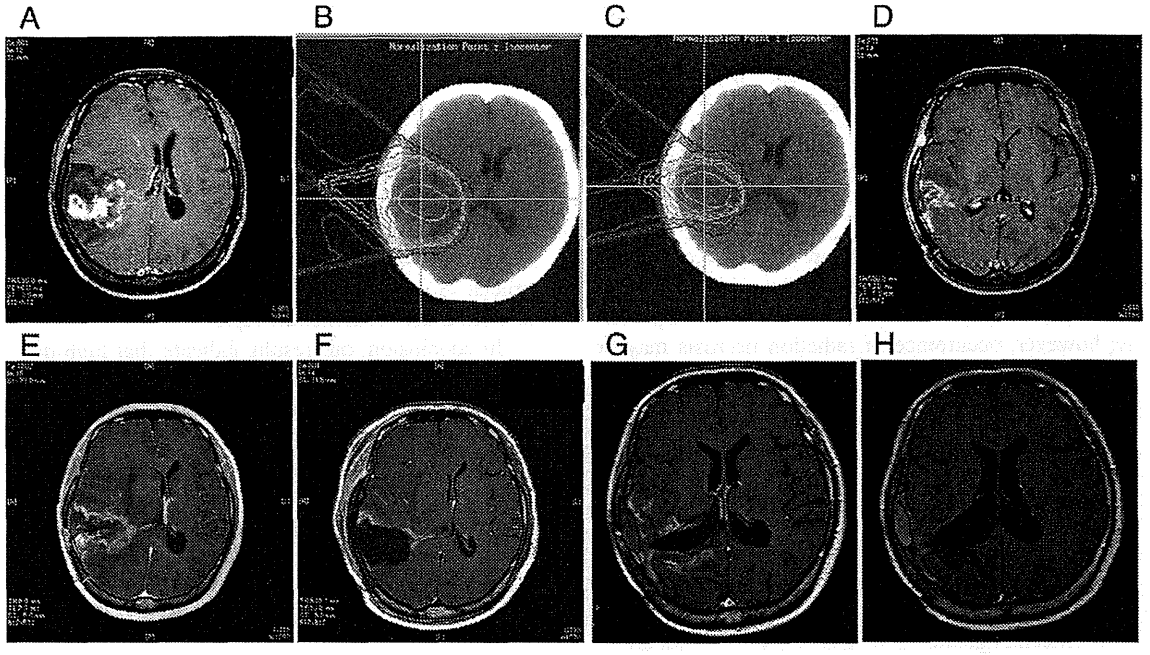

Figure 4 Case 1. Postcontrast T1-weighted magnetic resonance imaging (MRI) before the initial surgery (A). Isodose curves for proton beams representing 100%-10% of the prescribed dose at 10% intervals for the area of contrast enhancement on MRI plus a 10-mm margin (B) and for the area of contrast enhancement on MRI (C). Postcontrast T1-weighted MRI at 11 months after proton beam therapy (PBT) (D), at 20 months after PBT (E), after the second surgery (F), at 42 months after PBT (G), and at 51 months after PBT (H).

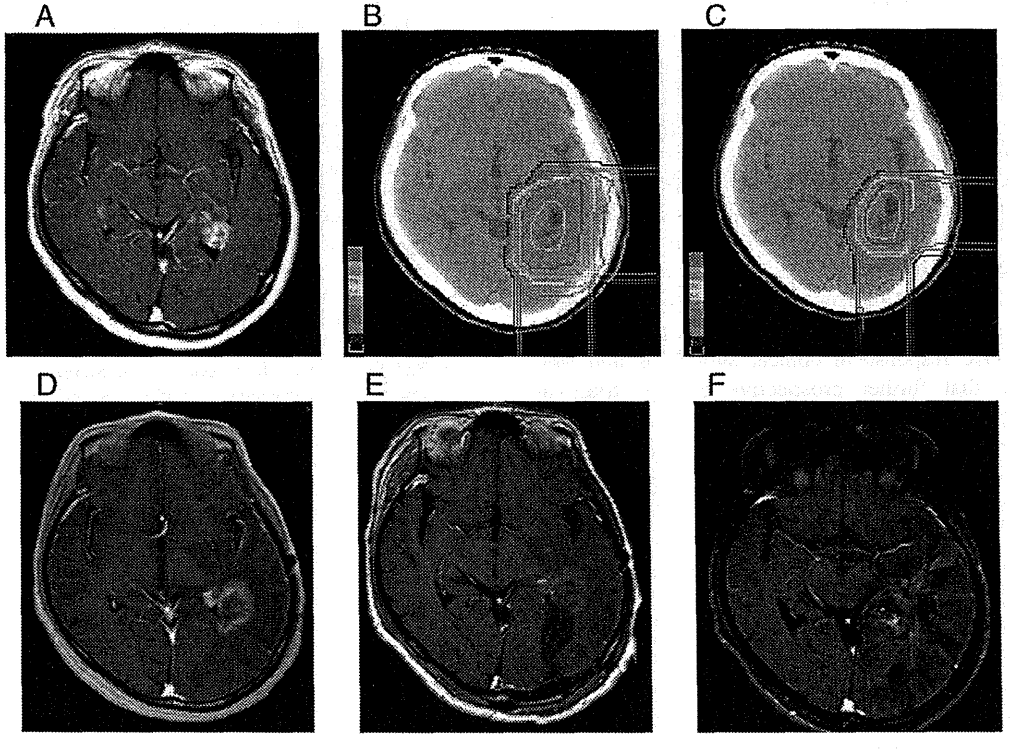

Figure 5 Case 2. Postcontrast T1-weighted magnetic resonance imaging (MRI) before the initial surgery (A). Isodose curves for proton beams representing 100%-10% of the prescribed dose at 10% intervals for the area of contrast enhancement on MRI plus a 10-mm margin (B) and for the area of contrast enhancement on MRI (C). Postcontrast T1-weighted MRI at 9 months after proton beam therapy (PBT) (D), after the second surgery (E), and at 40 months after PBT (F).

actual incidence of radiation necrosis in conventionally treated cases should be higher, although it has been reported that radiation necrosis of the brain occurs in approximately 5% of cases treated with 60 Gy x-ray radiation therapy.[20] Thus, radiation necrosis was observed in only 6 of our 23 patients (26%), maybe partly because of improved local control and subsequent prolonged survival with our treatment regimen.

Seizure or paralysis and coma are classified as grade 4 in the RTOG/EORTC late radiation morbidity scoring scheme.[12] Prevention of radiation necrosis is an important issue; however, occurrence of radiation necrosis may be inevitable using a 96.6 GyE protocol if long-term survival is achieved. We posit that the excellent dose concentricity of proton beams in our PBT method probably contributed to not only preservation of healthy brain tissue but also minimization of the volume of radiation necrosis. Moreover, we postulate that radiation necrosis could be more controllable and less fatal compared with GBM recurrence. In fact, our data showed that overall and MRI change-free survival in patients with radiation necrosis were significantly greater than those in patients with tumor recurrence. These findings are compatible with those of Rusthoven et al,[9] who found that patients with radiation necrosis at reoperation had improved survival compared with those with tumor recurrence in a study of grade 3-4 glioma treated with standard therapy.

Although necrotomy, hyperbaric oxygen therapy, anticoagulant therapy, and corticosteroid therapy have been used as treatments for radiation necrosis, a standard therapy has not yet been established.[21] At present, necrotomy is generally indicated for symptomatic radiation necrosis and 5 of the 6 patients who underwent necrotomy in our study had favorable outcomes. Recent reports suggest that bevacizumab, a monoclonal antibody to vascular endothelial growth factor, is effective for unresectable radiation necrosis.[22] On the basis of these reports, 2 patients in our series were treated with intravenous bevacizumab administration. Both patients showed good response in clinical symptoms and MRI, indicating that further prospective clinical trials are warranted for establishing bevacizumab as a treatment option for radiation necrosis.

Hypermethylation of the O6-methylguanine-DNA methyltransferase (MGMT) promoter is a favorable prognostic factor in GBM patients.[23] Minniti et al[24] found the rate of recurrence from the irradiated field was lower in cases with a methylated MGMT promoter region than in those with an unmethylated MGMT promoter region. Considering the present study did not examine the MGMT methylation status, further studies are needed to analyze the possible associations among MGMT promoter methylation, radiation necrosis, and long-term survival in GBM patients.

Our previously published retrospective data[25] showed that the median overall survival was 24.4 months (95% CI, 18.2-30.5 months) in 32 patients who received high-dose radiation therapy (the present treatment protocol or boron neutron capture therapy) compared with 14.2 months (95% CI, 10.0-18.3 months) in 35 patients treated with conventional radiation therapy (60.0-61.2 Gy in 30-34 fractions). Although KPS or tumor size in patients who received the above high-dose radiation therapy were favorable compared with the conventional cohort, we believe that dose escalation using modern treatment techniques is promising for improving GBM patient outcomes. Therefore, it is crucial to verify and optimize treatment indications using said high-dose radiation therapies.

In conclusion, our results indicate that high-dose 96.6 GyE concentric PBT has a high potential to improve survival in GBM patients if the treatment area completely covers the area of tumor infiltration. In addition, the remaining volume of healthy brain tissue was fairly well preserved in long-term survivors using our protocol. Although radiation necrosis is inevitable in the treated area, it may be controllable with necrotomy and bevacizumab administration.

References

1. Athanassiou H, Synodinou M, Maragoudakis E, et al. Randomized phase II study of temozolomide and radiotherapy compared with radiotherapy alone in newly diagnosed glioblastoma multiforme. *J Clin Oncol.* 2005;23:2372-2377.
2. Stupp R, Mason WP, van den Bent MJ, et al. Radiotherapy plus concomitant and adjuvant temozolomide for glioblastoma. *N Engl J Med.* 2005;352:987-996.
3. Moyal EC, Laprie A, Delannes M, et al. Phase I trial of tipifarnib (R115777) concurrent with radiotherapy in patients with glioblastoma multiforme. *Int J Radiat Oncol Biol Phys.* 2007;68:1396-1401.
4. Drappatz J, Norden AD, Wong ET, et al. Phase I study of vandetanib with radiotherapy and temozolomide for newly diagnosed glioblastoma. *Int J Radiat Oncol Biol Phys.* 2010;78:85-90.
5. Muragaki Y, Maruyama T, Iseki H, et al. Phase I/IIa trial of autologous formalin-fixed tumor vaccine concomitant with fractionated radiotherapy for newly diagnosed glioblastoma. *J Neurosurg.* 2011;115:248-255.
6. Fujii O, Soejima T, Kuwatsuka Y, et al. Supratentorial glioblastoma treated with radiotherapy: Use of the Radiation Therapy Oncology Group recursive partitioning analysis grouping for predicting survival. *Jpn J Clin Oncol.* 2010;40:726-731.
7. Fitzek MM, Thornton AF, Rabinov JD, et al. Accelerated fractionated proton/photon irradiation to 90 cobalt gray equivalent for glioblastoma multiforme: Results of a phase II prospective trial. *J Neurosurg.* 1999;91:251-260.
8. Tsien C, Moughan J, Michalski JM, et al. Phase I three-dimensional conformal radiation dose escalation study in newly diagnosed glioblastoma: Radiation Therapy Oncology Group Trial 98-03. *Int J Radiat Oncol Biol Phys.* 2009;73:699-708.
9. Rusthoven KE, Olsen C, Franklin W, et al. Favorable prognosis in patients with high-grade glioma with radiation necrosis: The University of Colorado reoperation series. *Int J Radiat Oncol Biol Phys.* 2011;81:211-217.
10. Mizumoto M, Tsuboi K, Igaki H, et al. Phase I/II trial of hyperfractionated concomitant boost proton beam therapy for supratentorial glioblastoma multiforme. *Int J Radiat Oncol Biol Phys.* 2010;77:98-105.

11. McDonald MW, Shu HK, Curran Jr WJ, Crocker IR. Pattern of failure after limited margin radiotherapy and temozolomide for glioblastoma. *Int J Radiat Oncol Biol Phys.* 2011;79:130-136.
12. Radiation Therapy Oncology Group. Available at: http://www.rtog.org/ResearchAssociates/AdverseEventReporting/RTOGEORTCLateRadiationMorbidityScoringSchema.aspx. Accessed July 20, 2013.
13. Knäusl B, Lütgendorf-Caucig C, Hopfgartner J, et al. Can treatment of pediatric Hodgkin's lymphoma be improved by PET imaging and proton therapy? *Strahlenther Onkol.* 2013;189:54-61.
14. Lorentini S, Amichetti M, Spiazzi L, et al. Adjuvant intensity-modulated proton therapy in malignant pleural mesothelioma. A comparison with intensity-modulated radiotherapy and a spot size variation assessment. *Strahlenther Onkol.* 2012;188:216-225.
15. Mizumoto M, Okumura T, Hashimoto T, et al. Proton beam therapy for hepatocellular carcinoma: A comparison of three treatment protocols. *Int J Radiat Oncol Biol Phys.* 2011;81:1039-1045.
16. Mizumoto M, Hashii H, Senarita M, et al. Proton beam therapy for malignancy in Bloom syndrome. *Strahlenther Onkol.* 2013;189:335-338.
17. Mizumoto M, Sugahara S, Nakayama H, et al. Clinical results of proton-beam therapy for locoregionally advanced esophageal cancer. *Strahlenther Onkol.* 2010;186:482-488.
18. Mizumoto M, Okumura T, Ishikawa E, et al. Reirradiation for recurrent malignant brain tumor with radiotherapy or proton beam therapy. *Strahlenther Onkol.* 2013;189:656-663.
19. Mizumoto M, Nakayama H, Tokita M, et al. Technical considerations for noncoplanar proton-beam therapy of patients with tumors proximal to the optic nerve. *Strahlenther Onkol.* 2010;186:36-39.
20. Ruben JD, Dally M, Bailey M, Smith R, McLean CA, Fedele P. Cerebral radiation necrosis: Incidence, outcomes, and risk factors with emphasis on radiation parameters and chemotherapy. *Int J Radiat Oncol Biol Phys.* 2006;65:499-508.
21. Bui QC, Lieber M, Withers HR, Corson K, van Rijnsoever M, Elsaleh H. The efficacy of hyperbaric oxygen therapy in the treatment of radiation-induced late side effects. *Int J Radiat Oncol Biol Phys.* 2004;60:871-878.
22. Levin VA, Bidaut L, Hou P, et al. Randomized double-blind placebo-controlled trial of bevacizumab therapy for radiation necrosis of the central nervous system. *Int J Radiat Oncol Biol Phys.* 2011;79:1487-1495.
23. Chandler KL, Prados MD, Malec M, Wilson CB. Long-term survival in patients with glioblastoma multiforme. *Neurosurgery.* 1993;32:716-720.
24. Minniti G, Amelio D, Amichetti M, et al. Patterns of failure and comparison of different target volume delineations in patients with glioblastoma treated with conformal radiotherapy plus concomitant and adjuvant temozolomide. *Radiother Oncol.* 2010;97:377-381.
25. Matsuda M, Yamamoto T, Ishikawa E, et al. Prognostic factors in glioblastoma multiforme patients receiving high-dose particle radiotherapy or conventional radiotherapy. *Br J Radiol.* 2011;84:54-60.

Journal of Radiation Research, 2014, 55, 803–811
doi: 10.1093/jrr/rru017 Advance Access Publication 27 March 2014

Inflammation as well as angiogenesis may participate in the pathophysiology of brain radiation necrosis

Erina YORITSUNE[1], Motomasa FURUSE[1], Hiroko KUWABARA[2], Tomo MIYATA[1], Naosuke NONOGUCHI[1], Shinji KAWABATA[1], Hana HAYASAKI[3], Toshihiko KUROIWA[1], Koji ONO[4], Yuro SHIBAYAMA[2] and Shin-Ichi MIYATAKE[1,*]

[1]Department of Neurosurgery, Division of Life Sciences, Osaka Medical College, 2-7 Daigaku-machi, Takatsuki City, Osaka 569-8686, Japan
[2]Department of Pathology, Division of Life Sciences, Osaka Medical College, 2-7 Daigaku-machi, Takatsuki City, Osaka 569-8686, Japan
[3]Department of Anatomy and Cell Biology, Division of Life Sciences, Osaka Medical College, 2-7 Daigaku-machi, Takatsuki City, Osaka 569-8686, Japan
[4]Particle Radiation Oncology Research Center, Research Reactor Institute, Kyoto University, Japan
*Corresponding author. Department of Neurosurgery, Osaka Medical College, 2-7 Daigaku-machi, Takatsuki City, Osaka 569-8686, Japan. Tel: +81-72-683-1221; Fax: +81-72-681-3723; Email: neu070@poh.osaka-med.ac.jp

(Received 13 September 2013; revised 14 February 2014; accepted 21 February 2014)

Radiation necrosis (RN) after intensive radiation therapy is a serious problem. Using human RN specimens, we recently proved that leaky angiogenesis is a major cause of brain edema in RN. In the present study, we investigated the same specimens to speculate on inflammation's effect on the pathophysiology of RN. Surgical specimens of symptomatic RN in the brain were retrospectively reviewed by histological and immunohistochemical analyses using hematoxylin and eosin (H&E) staining as well as immunohistochemical staining for VEGF, HIF-1α, CXCL12, CXCR4, GFAP, CD68, hGLUT5, CD45, IL-1α, IL-6 TNF-α and NF-*k*B. H&E staining demonstrated marked angiogenesis and cell infiltration in the perinecrotic area. The most prominent vasculature was identified as thin-walled leaky angiogenesis, i.e. telangiectasis surrounded by prominent interstitial edema. Two major cell phenotypes infiltrated the perinecrotic area: GFAP-positive reactive astrocytes and CD68/hGLUT5-positive cells (mainly microglias). Immunohistochemistry revealed that CD68/hGLUT5-positive cells and GFAP-positive cells expressed HIF-1α and VEGF, respectively. GFAP-positive cells expressed chemokine CXCL12, and CD68/hGLUT5-positive cells expressed receptor CXCR4. The CD68/hGLUT5-positive cells expressed pro-inflammatory cytokines IL-1α, IL-6 and TNF-α in the perinecrotic area. VEGF caused leaky angiogenesis followed by perilesional edema in RN. GFAP-positive cells expressing CXCL12 might attract CXCR4-expressing CD68/hGLUT5-positive cells into the perinecrotic area. These accumulated CD68/hGLUT5-positive cells expressing pro-inflammatory cytokines seemed to aggravate the RN edema. Both angiogenesis and inflammation might be caused by the regulation of HIF-1α, which is well known as a transactivator of VEGF and of the CXCL12/CXCR4 chemokine axis.

Keywords: brain radiation necrosis; CXCL12/CXCR4 chemokine axis; inflammation; microglia; pro-inflammatory cytokine

INTRODUCTION

Radiotherapeutic technologies have progressed in recent decades; patients with malignant brain tumors can now be treated with high-dose irradiation with good conformity, prolonging their survival. On the other hand, brain radiation necrosis (RN), a late adverse effect of radiation therapies, has become a serious problem, and existing treatments for brain RN have not been sufficiently effective. Recently, bevacizumab (BV), an antibody to vascular endothelial growth factor (VEGF), has received attention as a promising treatment for RN [1–3]. BV shows sharp and potent treatment effects. On

the basis of our analysis of human RN surgical specimens, we previously demonstrated that edema in RN is caused by VEGF overexpression in reactive astrocytes [4]. However, the effects are often temporary; RN occasionally recurs after BV treatments [1]. Therefore, to overcome this intractable pathology, it will be necessary to elucidate its underlying mechanisms.

In a recent study using human RN specimens, we proved that 'leaky' angiogenesis is a major cause of brain edema in RN [4], as shown in Fig. 1 in this report. Furthermore, we have discovered that GFAP-positive and CD68-positive cells accumulate around the circumference of the RN core, i.e. the perinecrotic area [5]. In addition, we have shown that HIF-1α and VEGF participate in the formation of angiogenesis, microbleeding, and interstitial edema at the RN circumference [4]. However, it remains to be determined why these GFAP-positive cells and CD68-positive cells accumulate in the perinecrotic area, which cells express VEGF and HIF-1α in RN, and whether or not other molecules participate in the pathophysiology of RN.

In malignant tumors (including glioblastomas) the CXCL12/CXCR4 chemokine axis is known to be correlated with HIF-1α and VEGF expression [6, 7]. Furthermore, the involvement of chronic inflammation has also been suggested as a mechanism (in addition to angiogenesis) underlying brain RN [8]. The aim of the present study is to elucidate the molecular mechanisms underlying brain RN in humans, with special reference to angiogenesis and inflammation. We also speculated on the potential relationship between chemokine and cytokine expression and accumulation in GFAP, CD68, hGLUT5 and CD45-positive cells in the perinecrotic area. Here, GFAP, CD68, hGLUT5 and CD45 were adopted as markers for astrocytes, monocytes, microglias and lymphocytes, respectively. The study design consisted of a retrospective qualitative review with histological and immunohistochemical analyses of surgical specimens from the brains of patients with symptomatic RN treated in our department.

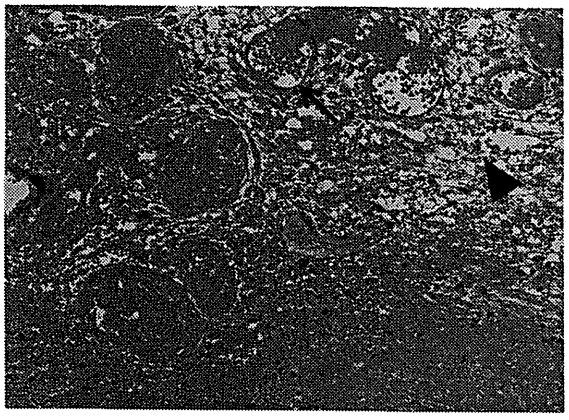

Figure 1. A hematoxylin and eosin (H&E)-stained specimen from Case 5. Thin-walled enlarged capillaries indicating telangiectasis (arrow) and the proliferation of arterioles can be seen in the area between the necrotic core and normal brain tissue. These blood vessels were accompanied by interstitial edema (arrowhead) due to plasma leakage. The original objective magnification was ×100.

MATERIALS AND METHODS

Specimens

Surgical specimens of seven patients with symptomatic RN in the brain who had been treated in our department from 2006 through 2009 were subjected to histological and immunohistochemical analyses. The study was approved by the Osaka Medical College Ethics Committee, and we obtained informed consent from all of the patients prior to surgeries and procedures. All of the patients had received radiation therapy, including X-ray treatment, stereotactic radiosurgery (SRS), and/or boron neutron capture therapy [9–13]. They also had received some medical treatments for RN, including corticosteroids, anticoagulants, and so on, for at least one month; however, the symptoms were refractory to these medical treatments. The original diseases were two head and neck cancers, four glioblastomas, and one metastatic brain tumor derived from breast cancer. Both patients with head and neck cancers had only extracranial tumors without infiltration and/or metastasis to the brain. Their irradiation fields included not only the original head and neck cancers but also some part of the temporal lobe. Therefore, these were samples of pure RN without the presence of tumor cells in the temporal lobe. Brain RN in all cases was diagnosed by pathological examination of the surgical specimen (Table 1).

Tissue preparation and immunohistochemistry

Tissue samples were fixed in 10% buffered formalin and embedded in paraffin. Tissue sections were cut (4-μm slices), deparaffinized with xylene, and rehydrated through graduated ethanol solutions. One section of each sample was stained with hematoxylin and eosin (H&E), and the other sections were used for HIF-1α, VEGF, CXCL12, CXCR4, IL-1α, IL-6, TNF-α, GFAP, CD68, hGLUT5, CD45 and NF-κB staining by the biotin–streptavidin–peroxidase method. Here, GFAP, CD68, hGLUT5 and CD45 were adopted as markers for astrocytes, monocytes, microglias and lymphocytes, respectively, as described above. Deparaffinized and rehydrated sections were subjected to pressure boiling for antigen retrieval in antigen unmasking solution. These sections were incubated with 0.03% hydrogen peroxidase for 5 min at room temperature to block endogenous peroxidase activity. The sections were then incubated with one of the above 12 primary antibodies at 4°C overnight. The information on these primary antibodies, including dilutions, is summarized in Table s1. The sections were then incubated with peroxidase-labeled secondary antibody (Dako) for 30 min at room temperature.

Table 1. Patient profile of symptomatic radiation necrosis

Case	Age	Gender	Original dis.[a]	Radiation[b]	Duration[c]	Chemotherapy[d]
1	78	M	Sal. Duc. Ca.	XRT (60 Gy), BNCT × 2 (6.1 and 10.1 Gy-Eq)	20	
2	46	F	Ade. Ca.	XRT (60 Gy), BNCT × 2 (6.9 and 6.7 Gy-Eq)	7	MTX, UFT, CDDP
3	69	F	GB	XRT (60 Gy), BNCT (13.3 Gy-Eq)	3	ACNU
4	68	F	GB	XRT (60 Gy), BNCT (9.67 Gy-Eq)	12	
5	46	M	GB	XRT (60 Gy), BNCT (13.7 Gy-Eq)	5	PCV
6	39	M	GB	XRT (60 Gy), SRS (18 Gy)	8	ACNU
7	54	F	Ade. Ca.	SRS (22 Gy)	9	Herceptin

[a]Sal. Duc. Ca. = salivary ductal carcinoma, GB = glioblastoma, Ade. Ca. = adenocarcinoma. [b]XRT = X-ray treatment, BNCT = boron neutron capture therapy, SRS = stereotactic radiosurgery, Gy-Eq = biologically equivalent X-ray dose that would have equivalent effects on tumor and normal brain. In BNCT, the presented dose is the peak point dose for normal brain. In SRS, the presented dose is the marginal X-ray or gamma-ray dose. BNCT × 2 means intentional fractionated BNCT in two sessions. [c]Months between termination of last radiotherapy and onset of symptoms caused by radiation necrosis. Radiation necrosis in Cases 1 and 2 occurred in temporal lobes and was included in the irradiation fields. [d]MTX = methotrexate, UFT = combined drug of tegafur and uracil, CDDP = cisplatin, ACNU = nimustin, PCV = procarbazine, nimustin, vincristine.

They were developed with diaminobenzidine, lightly counterstained with hematoxylin, and mounted.

Double immunofluorescence microscopy

Double immunofluorescence staining was performed using the following antibody combinations: CXCL12 and GFAP or CD68, CXCR4 and GFAP or CD68, HIF-1α and GFAP or CD68, VEGF and GFAP or CD68, IL-1α and GFAP or CD68, IL-6 and GFAP or CD68, TNF-α and GFAP or CD68, hGLUT5 and CD68 or CXCR4 or IL-1α or HIF-1α, and CD45 and IL-1α or CXCR4. The secondary antibodies used were Alexa Fluor 488 goat anti-mouse IgG, Alexa Fluor 488 goat anti-rabbit IgG, Alexa Fluor 546 goat anti-mouse IgG, and Alexa Fluor 546 goat anti-rabbit IgG (Invitrogen, Carlsbad, CA). These were examined using an LSM510 laser scanning confocal microscope (Carl Zeiss, Oberkochen, Germany).

RESULTS

Histochemical analysis with H&E staining

Figure 1 shows a typical finding of H&E staining of RN from Case 5. Remarkable angiogenesis existed in the perinecrotic area. The most prominent vasculature was identified as a thin-walled, leaky angiogenesis, such as telangiectasis with prominent interstitial edema, which is consistent with our previous study [4]. The interstitial edema was probably caused by leakage of the plasma from the fragile angiogenesis. There was no cytoarchitecture in the core of the necrotic foci, whereas some infiltrating cells were observed in the perinecrotic area, as indicated with hematoxylin-stained nuclei. Of course, the incidence of RN is generally affected by the applied radiation dose, distribution, and adjuvant chemotherapy [14, 15]. However, these are universal pathological findings, irrespective of the original tumor types and radiation modalities, as we reported previously [4].

Immunohistochemical analysis of the localization of CXCL12, CXCR4, GFAP, CD68, IL-1α, IL-6, TNF-α, NF-κB, hGLUT5 and CD45

We next sought to determine the cell types (i.e. astrocytes or monocytes) that produce chemokines and/or express the corresponding receptors. To this end, we performed enzyme-immunohistochemical analyses for gross identification of the infiltrative cells and proteins expressed using the primary antibodies described in Materials and Methods. H&E staining was also performed on each specimen to identify the necrotic core, the perinecrotic area, and the normal brain area. The specimens obtained from Cases 2 and 3 demonstrate representative findings for the expression of GFAP, CD68, CXCL12 and CXCR4 (Fig. 2). As we reported previously [5], two major cell phenotypes infiltrated the perinecrotic area: GFAP-positive astrocytes and CD68-positive monocytes. We observed similar distributions of GFAP-positive cells and CXCL12-positive cells; CD68-positive cells and CXCR4-positive cells were also similarly distributed. The former cell type was limited mainly to the perinecrotic area, whereas the latter population was observed not only in the perinecrotic area but also, though to a lesser degree, in the necrotic core. The same tendencies were observed among all cases (data not shown).

To evaluate the distribution of cytokine production in RN, we performed immunohistochemical staining for IL-1α, IL-6 and TNF-α. The specimens obtained from all cases revealed oval cells positive for IL-1α, IL-6 and TNF-α in the perinecrotic area (data not shown). These cells also appeared inside the necrotic

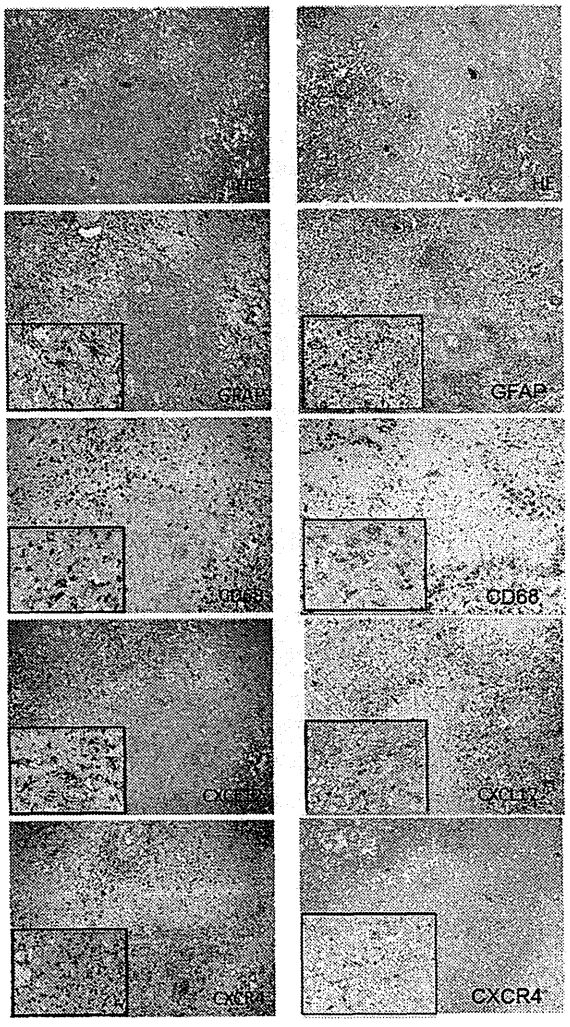

Figure 2. H&E staining and immunohistochemistry for GFAP, CD68, CXCL12 and CXCR4 of the surgical specimen from Case 2 in the left column and for Case 3 in the right column. H&E staining showed the necrotic core and the surrounding tissue (perinecrotic area). Immunohistochemical staining for GFAP, CD68, CXCL12 and CXCR4 revealed GFAP- and CXCL12-positive astrocytic cells, and CD68- and CXCR4-positive oval cells in the perinecrotic area. CD68- and CXCR4-positive cells were also observed in small numbers inside the necrotic core. On the other hand, no or scarce immunoreactivity of GFAP and CXCL12 was observed in the necrotic core. The original objective magnifications were ×40 and ×200.

core, though to a lesser degree. We then examined the expression of NF-κB as a master molecule of inflammation in RN using the Case 2 specimens. Interestingly, NF-κB was expressed not in normal brain tissue but in the perinecrotic area (Fig. *s*1). This molecule was expressed not only in the cytoplasm but also in the nucleus, and was morphologically assessed as a monocyte. The same tendency was confirmed in Case 3.

Subsequently, we focused on immune cells in the brain to determine their effect on RN. To this end, we performed an immunohistochemical study using hGLUT5, CD68 and CD45 antibodies, as stated above. We observed similar distributions in hGLUT5-positive cells and CD68-positive cells in Cases 3 and 4 (Fig. *s*2). However, the number of CD45-positive cells was limited; their distribution pattern was distinguishable from those of GFAP-positive cells and CD68- and hGLUT5-positive cells. The same tendencies were observed in Cases 6 and 7 (data not shown).

Taken together, these data suggested that CXCL12 and CXCR4 might be expressed in GFAP-positive reactive astrocytes and hGLUT5- and/or CD68-positive cells, respectively. Also, microglias, macrophages, and even lymphocytes, each of which can produce proinflammatory cytokines, accumulated in the perinecrotic area. Therefore, inflammation might play a significant role in the pathogenesis of RN in the brain.

Relationships between CXCL12, CXCR4, HIF-1α, VEGF, IL-1α, IL-6 and TNF-α expression and GFAP/CD68 expression in radiation necrosis

In order to further examine the distribution of cells responsible for the expression of cytokines and chemokines, we performed double immunofluorescence staining. The specimen from Case 2 provided a representative pattern (Figs 3 and 4). Figure 3 shows that the expression of HIF-1α was recognized not in GFAP-positive cells (a) but in most CD68-positive cells (b). However, some CD68-positive cells did not produce HIF-1α, while some CD68-negative cells did. VEGF was expressed in GFAP-positive cells (c) but was hardly expressed in CD68-positive cells (d). Likewise, the expression of CXCL12 was detected in GFAP-positive cells (e) but not in CD68-positive cells (f). In contrast, CXCR4 was not expressed in GFAP-positive cells (g) but was expressed in CD68-positive cells (h). However, some CXCR4 expression was recognized in CD68-negative cells.

Furthermore, Fig. 4 shows that IL-1α, IL-6 and TNF-α were not expressed in GFAP-positive cells (a, c, e) but were expressed in CD68-positive cells (b, d, f). The same tendencies were confirmed in the other specimens (data not shown).

Relationships between CXCR4, HIF-1α and IL-1α expression and hGLUT5/CD68 and CD45 expression in radiation necrosis

In order to identify the cells that are responsible for inflammation in RN, we analyzed double immunofluorescence using anti-CD68, anti-hGLUT5 and anti-CD45 antibodies. We used the former two antibodies to distinguish microglias from macrophages originating from peripheral blood in CD68-positive cells. Figure *s3* (Case 1) shows that CXCR4, HIF-1α and IL-1α were expressed in many hGLUT5-positive cells (a, b, c). However, some CXCR4, HIF-1α and IL-1α-positive cells did not express hGLUT5 and vice versa. Also, most CD68-positive cells were identical to hGLUT5-positive cells,

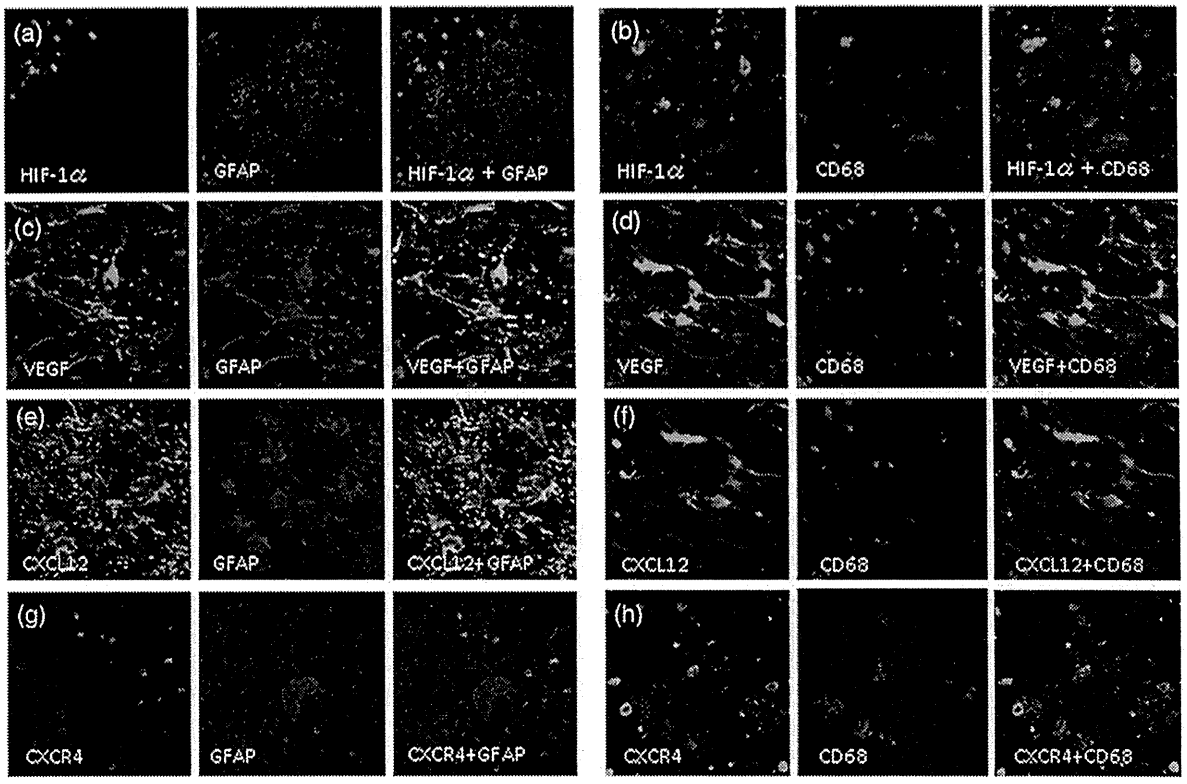

Figure 3. Double immunofluorescence staining of the specimen from Case 2. The expression of HIF-1α was not detected in reactive astrocytes, as revealed by GFAP (**a**), but was detected in CD68-positive cells (**b**). VEGF was expressed in GFAP-positive cells (**c**) but was hardly expressed in CD68-positive cells (**d**). Similarly, CXCL12 was expressed in GFAP-positive reactive astrocytes (**e**) but not in CD68-positive cells (**f**). In contrast, CXCR4 was not expressed in GFAP-positive cells (**g**) but was expressed in CD68-positive cells (**h**). The original objective magnification was ×400.

although some cells expressed only CD68 or hGLUT5 (d). Almost no CD45-positive cells produced IL-1α. Interestingly, almost all CD45-positive cells co-expressed CXCR4 (data not shown). This is confirmed in the other cases.

DISCUSSION

Medical treatment with the anti-VEGF antibody BV, or surgical resection of necrotic tissue containing VEGF-producing cells may serve to decrease perilesional edema and immediately improve symptoms stemming from the efficient reduction of VEGF in the perinecrotic area [1–3, 5]. These phenomena suggest that VEGF is the key molecule in the pathogenesis of RN. Here the role of reactive astrocytes in RN is clearly the production of VEGF, while that of monocytes remains unclear. The present results prove that these monocytes in the perinecrotic area produce HIF-1α. HIF-1α is a well-known transactivator not only for VEGF, but also for the CXCL12-CXCR4 axis [6, 7, 16]. The CXCL12-CXCR4 axis is also well known to be a chemotactic factor and to play a significant role in inflammation. Therefore, we examined the expression of these molecules in RN. As we had speculated, CXCR4-positive monocytes and lymphocytes gathered in the perinecrotic area.

Yoshii *et al.* stressed the mechanism underlying the development and progress of late cerebral RN, with special emphasis on inflammatory responses [8]. They put forward the following hypothesis to explain the mechanism underlying RN. First, irradiation damages endothelial cells, causing the blood–brain barrier (BBB) to fail. The inflammatory cells then cross into the extravascular space. At the same time, these cells secrete cytokines that cause other inflammatory cells to develop. This effect becomes an uncontrolled inflammatory response and continues, becoming chronic inflammation [8]. Thereafter we examined the role of inflammation in RN more precisely by using immunohistochemistry and double immunofluorescence. Kureshi *et al.* reported that macrophages and some astrocytes might migrate to the RN area and produce IL-1α, TNF-α and IL-6 [17]; this would be partly consistent with our present results, although the exact cell types corresponding to each type of cytokine production were ambiguous in their report. In laboratory animal RN

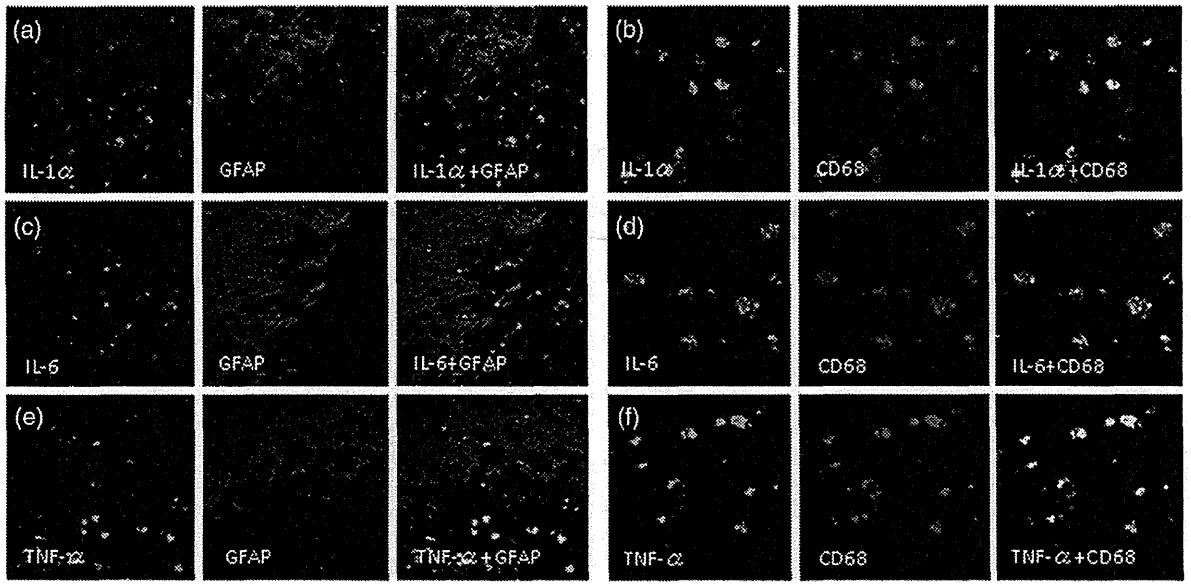

Figure 4. Double immunofluorescence staining of Case 2. IL-1α, IL-6 and TNF-α were not expressed in reactive astrocytes, as revealed by GFAP-positive cells (**a, c, e**), but were expressed in CD68-positive cells (**b, d, f**). The original objective magnification was ×400.

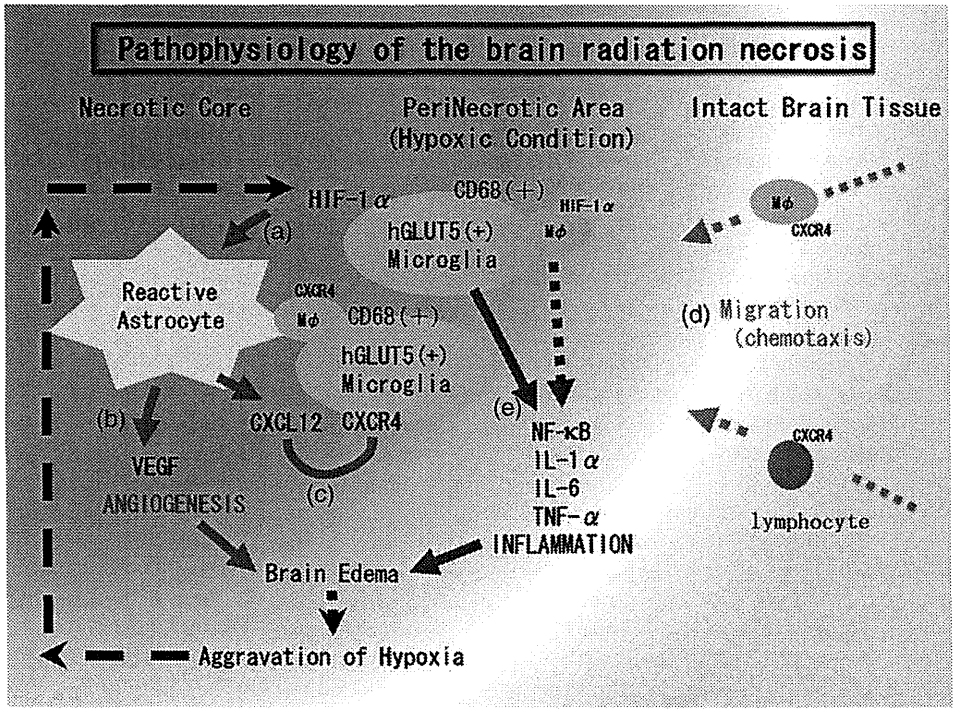

Figure 5. Hypothesis of the pathophysiology of brain radiation necrosis. (**a**) Vascular damage around the irradiated tumor tissue caused tissue ischemia. This hypoxia induced hGLUT5-positive microglias to express HIF-1α around the necrotic core. (**b**) Under HIF-1α regulation, VEGF was expressed in reactive astrocytes, causing leaky and fragile angiogenesis. (**c**) CXCL12/CXCR4 signaling is also regulated by HIF-1α. (**d**) CXCL12-expressing reactive astrocytes might draw CXCR4-expressing macrophages and lymphocytes by chemotaxis into the perinecrotic area. (**e**) These accumulated hGLUT5-positive microglias producing NF-κβ and pro-inflammatory cytokines seemed to aggravate radiation necrosis.

models, a key cytokine is TNF-α, which regulates other pro-inflammatory cytokines to increase BBB permeability and leukocyte adhesion, to activate astrocytes, and to induce endothelial apoptosis [18–21]. Moreover, IL-1α, either alone or in cooperation with TNF-α and IL-6 in the downstream region, exacerbates inflammation [22].

The roles of chemokine CXCL12 and its receptor CXCR4 have been well established in the immune and nervous systems, where they localize in various cell types with specific microenvironments [23]. CXCR4 is expressed not only in monocytes, but also in lymphocytes [24, 25]. In the present study, CD45-positive cells expressed CXCR4, as described in Results. Thereafter, these lymphocytes might be drawn into the perinecrotic area from peripheral blood by homing; however, unlike CD68- and/or hGLUT5-positive cells, they did not produce pro-inflammatory cytokines. At first, in this study, we used CD68 antibody to detect monocytes. But it was difficult for us to discriminate microglia from a macrophage in brain tissue using only this marker. Horikoshi and Sasaki *et al.* reported that the hGLUT5 antibody is a good and specific marker for microglia [26–32]. We therefore used it to recognize microglia. In the present study, CD68 and hGLUT5 were usually expressed in many identical cells, although some hGLUT5-positive cells did not show CD68 expression and vice versa. HIF-1α, CXCR4 and IL-1α expression was confined largely to hGLUT5-positive cells, but some of them were expressed in CD68-positive and hGLUT-5–negative cells, as stated in Results. Also, as described above, CD45 cells in the perinecrotic area expressed CXCR4 but not inflammatory cytokine. Taken together, these findings suggest that microglia play a key role in this inflammation, but some macrophages from peripheral blood may also be involved. However, lymphocytes do not participate in the production of pro-inflammatory cytokines.

We also examined NF-κB expression in the perinecrotic area (Fig. *s*1). At a glance, this molecule was expressed in monocytes in the perinecrotic area. NF-κB is well known as a major molecule of inflammation. As the function of NF-κB in RN is unclear, further examination is needed to elucidate this molecule's function. In culture conditions, CXCR4-positive microglia can produce IL-6 with CXCL12 stimuli via an NF-κB-dependent pathway [33]. This may suggest a role of NF-κB in RN. Also, it is observed in cerebral ischemia that CXCL12 is upregulated under ischemic conditions, thereby inducing monocytes to gather in the ischemic penumbra and a subsequent inflammatory response [34–36]. These observations support chemokine–cytokine interaction in RN.

From the observed qualitative data in this study, let us summarize our original hypothesis about RN pathophysiology (Fig. 5). That is, the first step in a brain undergoing radiation therapy and developing necrosis is blood vessel damage just around the tumor. This is connected with hypoxia close to the irradiated tumor tissue, which causes the upregulation of HIF-1α in hGLUT5-positive microglias. Because HIF-1α is well known as a transactivator of VEGF and CXCL12/CXCR4 signaling [7, 16], the upregulation of HIF-1α augments VEGF and CXCL12 expression in GFAP-positive reactive astrocytes. The former produced the leaky and fragile angiogenesis and the subsequent perilesional edema in RN. The latter might draw CXCR4-expressing hGLUT5-positive microglias and CXCR4-expressing lymphocytes by chemotaxis to the perinecrotic area. The production of pro-inflammatory cytokines by these accumulated hGLUT5-positive cells seemed to aggravate the perilesional edema. However, although some CD45-positive lymphocytes gathered in the perinecrotic area, they were not involved in pro-inflammatory cytokine production. NF-κB must play a significant role in RN inflammation. The aggravation of edema could lead to the further development of focal ischemia, which augments the expression of HIF-1α in the microglias in the perinecrotic area. Here, both angiogenesis and inflammation may contribute to a synergistic and malignant RN cycle. These hypotheses need to be confirmed in experimental animal models, as described below. In any case, the present results suggest that inflammation participates in the pathophysiology of brain RN.

The present research appears to have elucidated a part of the molecular mechanism underlying brain RN on the basis of qualitative histology and immunohistochemistry. In order to prove these hypotheses more conclusively, it will be necessary to create a brain RN model in laboratory animals and to analyze the pathophysiology in each stage. An improved understanding of the mechanism by which the numerous cytokines in brain RN are regulated could play an important role in the formulation of treatment strategies. If a brain RN becomes controllable, it will further advance the application of radiation therapy to central nervous system tumors, leading to the conquest of intractable malignant brain tumors. Furthermore, the quality of life of patients would certainly be improved by an effective treatment for symptomatic RN of the brain.

SUPPLEMENTARY DATA

Three supplementary figures (Figs *s*1, *s*2 and *s*3), one supplementary table (Table *s*1), and an appendix are available at the *Journal of Radiation Research* online.

ACKNOWLEDGEMENTS

This work was supported in part by a Grant-in-Aid for Scientific Research (B) (23390355) and by a Grant-in-Aid for Exploratory Research (24659658) to S-I.M., and by a Grant-in-Aid for Scientific Research (C) (23592145) to M.F. from the Japanese Ministry of Education, Culture, Sports, Science, and Technology. We thank Itsuko Inoue, Kaname Shimokawa and Shizuka Akashi for their technical assistance. We also thank Prof. Kazuhito Tomizawa (Department of Molecular Physiology, Kumamoto University), Dr Mitsugu Fujita (Department of Microbiology and Neurosurgery, Kinki

University Graduate School of Medical Sciences) and Dr Satoshi Kokura (Department of Molecular Gastroenterology and Hepatology, Kyoto Prefectural University of Medicine) for their critical reading and fruitful discussions concerning this manuscript.

FUNDING

Funding to pay Open Access publication charges for this article was provided by a Grant-in-Aid for Scientific Research (B) (23390355) and by a Grant-in-Aid for Exploratory Research (24659658) to S-I.M., and by a Grant-in-Aid for Scientific Research (C) (23592145) to M.F. from the Japanese Ministry of Education, Culture, Sports, Science, and Technology.

REFERENCES

1. Furuse M, Kawabata S, Kuroiwa T *et al.* Repeated treatments with bevacizumab for recurrent radiation necrosis in patients with malignant brain tumors: a report of 2 cases. *J Neurooncol* 2011;**102**:471–5.
2. Gonzalez J, Kumar AJ, Conrad CA *et al.* Effect of bevacizumab on radiation necrosis of the brain. *Int J Radiat Oncol Biol Phys* 2007;**67**:323–6.
3. Levin VA, Bidaut L, Hou P *et al.* Randomized double-blind placebo-controlled trial of bevacizumab therapy for radiation necrosis of the central nervous system. *Int J Radiat Oncol Biol Phys* 2011;**79**:1487–95.
4. Nonoguchi N, Miyatake S, Fukumoto M *et al.* The distribution of vascular endothelial growth factor-producing cells in clinical radiation necrosis of the brain: pathological consideration of their potential roles. *J Neurooncol* 2011;**105**:423–31.
5. Miyatake S, Kuroiwa T, Kajimoto Y *et al.* Fluorescence of non-neoplastic, magnetic resonance imaging-enhancing tissue by 5-aminolevulinic acid: case report. *Neurosurgery* 2007;**61**: E1101–3; discussion E1103–4.
6. Kryczek I, Wei S, Keller E *et al.* Stroma-derived factor (SDF-1/CXCL12) and human tumor pathogenesis. *Am J Physiol Cell Physiol* 2007;**292**:C987–95.
7. Liang Z, Brooks J, Willard M *et al.* CXCR4/CXCL12 axis promotes VEGF-mediated tumor angiogenesis through Akt signaling pathway. *Biochem Biophys Res Commun* 2007;**359**:716–22.
8. Yoshii Y. Pathological review of late cerebral radionecrosis. *Brain Tumor Pathol* 2008;**25**:51–8.
9. Kawabata S, Miyatake S, Kuroiwa T *et al.* Boron neutron capture therapy for newly diagnosed glioblastoma. *J Radiat Res* 2009;**50**:51–60.
10. Miyatake S, Kawabata S, Kajimoto Y *et al.* Modified boron neutron capture therapy for malignant gliomas performed using epithermal neutron and two boron compounds with different accumulation mechanisms: an efficacy study based on findings on neuroimages. *J Neurosurg* 2005;**103**:1000–9.
11. Miyatake S, Kawabata S, Nonoguchi N *et al.* Pseudoprogression in boron neutron capture therapy for malignant gliomas and meningiomas. *Neuro-Oncology* 2009;**11**:430–6.
12. Miyatake S, Kawabata S, Yokoyama K *et al.* Survival benefit of Boron neutron capture therapy for recurrent malignant gliomas. *J Neurooncol* 2009;**91**:199–206.
13. Miyatake S, Tamura Y, Kawabata S *et al.* Boron neutron capture therapy for malignant tumors related to meningiomas. *Neurosurgery* 2007;**61**:82–90; discussion 90–1.
14. Ruben JD, Dally M, Bailey M *et al.* Cerebral radiation necrosis: incidence, outcomes, and risk factors with emphasis on radiation parameters and chemotherapy. *Int J Radiat Oncol Biol Phys* 2006;**65**:499–508.
15. de Wit MC, de Bruin HG, Eijkenboom W *et al.* Immediate post-radiotherapy changes in malignant glioma can mimic tumor progression. *Neurology* 2004;**63**:535–7.
16. Maxwell PH, Wiesener MS, Chang GW *et al.* The tumour suppressor protein VHL targets hypoxia-inducible factors for oxygen-dependent proteolysis. *Nature* 1999;**399**:271–5.
17. Kureshi SA, Hofman FM, Schneider JH *et al.* Cytokine expression in radiation-induced delayed cerebral injury. *Neurosurgery* 1994;**35**:822–9; discussion 829–30.
18. Ansari R, Gaber MW, Wang B *et al.* Anti-TNFA (TNF-alpha) treatment abrogates radiation-induced changes in vascular density and tissue oxygenation. *Radiat Res* 2007;**167**:80–6.
19. Mantych GJ, James DE, Devaskar SU. Jejunal/kidney glucose transporter isoform (Glut-5) is expressed in the human blood–brain barrier. *Endocrinology* 1993;**132**:35–40.
20. Siu A, Wind J, Iorgulescue J *et al.* Radiation necrosis following treatment of high grade glioma—a review of the literature and current understanding. *Acta Neurochir* 2012;**154**:191–201.
21. Wilson CM, Gaber MW, Sabek OM *et al.* Radiation-induced astrogliosis and blood-brain barrier damage can be abrogated using anti-TNF treatment. *Int J Radiat Oncol Biol Phys* 2009;**74**:934–41.
22. Nakae S, Saijo S, Horai R *et al.* IL-17 production from activated T cells is required for the spontaneous development of destructive arthritis in mice deficient in IL-1 receptor antagonist. *Proc Natl Acad Sci U S A* 2003;**100**:5986–90.
23. McCandless EE, Wang Q, Woerner BM *et al.* CXCL12 limits inflammation by localizing mononuclear infiltrates to the perivascular space during experimental autoimmune encephalomyelitis. *J Immunol* 2006;**177**:8053–64.
24. Cristillo AD, Highbarger HC, Dewar RL *et al.* Up-regulation of HIV coreceptor CXCR4 expression in human T lymphocytes is mediated in part by a cAMP-responsive element. *FASEB J* 2002;**16**:354–64.
25. Forster R, Kremmer E, Schubel A *et al.* Intracellular and surface expression of the HIV-1 coreceptor CXCR4/fusin on various leukocyte subsets: rapid internalization and recycling upon activation. *J Immunol* 1998;**160**:1522–31.
26. Burant CF, Takeda J, Brot-Laroche E *et al.* Fructose transporter in human spermatozoa and small intestine is GLUT5. *J Biol Chem* 1992;**267**:14523–6.
27. Gould GW, Holman GD. The glucose transporter family: structure, function and tissue-specific expression. *Biochem J* 1993;**295**:329–41.
28. Horikoshi Y, Sasaki A, Taguchi N *et al.* Human GLUT5 immunolabeling is useful for evaluating microglial status in neuropathological study using paraffin sections. *Acta Neuropathol* 2003;**105**:157–62.
29. Joost HG, Thorens B. The extended GLUT-family of sugar/polyol transport facilitators: nomenclature, sequence

characteristics, and potential function of its novel members (review). *Mol Membr Biol* 2001;**18**:247–56.
30. Kayano T, Burant CF, Fukumoto H *et al.* Human facilitative glucose transporters. Isolation, functional characterization, and gene localization of cDNAs encoding an isoform (GLUT5) expressed in small intestine, kidney, muscle, and adipose tissue and an unusual glucose transporter pseudogene-like sequence (GLUT6). *J Biol Chem* 1990;**265**:13276–82.
31. Mayhan WG. Cellular mechanisms by which tumor necrosis factor-alpha produces disruption of the blood–brain barrier. *Brain Res* 2002;**927**:144–52.
32. Sasaki A, Horikoshi Y, Yokoo H *et al.* Antiserum against human glucose transporter 5 is highly specific for microglia among cells of the mononuclear phagocyte system. *Neurosci Lett* 2003;**338**:17–20.
33. Lu DY, Tang CH, Yeh WL *et al.* SDF-1alpha up-regulates interleukin-6 through CXCR4, PI3 K/Akt, ERK, and NF-kappaB-dependent pathway in microglia. *Eur J Pharmacol* 2009;**613**:146–54.
34. Cruz-Orengo L, Holman DW, Dorsey D *et al.* CXCR7 influences leukocyte entry into the CNS parenchyma by controlling abluminal CXCL12 abundance during autoimmunity. *J Exp Med* 2011;**208**:327–39.
35. Hill WD, Hess DC, Martin-Studdard A *et al.* SDF-1 (CXCL12) is upregulated in the ischemic penumbra following stroke: association with bone marrow cell homing to injury. *J Neuropathol Exp Neurol* 2004;**63**:84–96.
36. Huang J, Li Y, Tang Y *et al.* CXCR4 antagonist AMD3100 protects blood–brain barrier integrity and reduces inflammatory response after focal ischemia in mice. *Stroke* 2013;**44**:190–7.

Biomaterials 35 (2014) 3396–3405

Contents lists available at ScienceDirect

Biomaterials

journal homepage: www.elsevier.com/locate/biomaterials

The acceleration of boron neutron capture therapy using multi-linked mercaptoundecahydrododecaborate (BSH) fused cell-penetrating peptide

Hiroyuki Michiue [a,*], Yoshinori Sakurai [b], Natsuko Kondo [b], Mizuki Kitamatsu [c], Feng Bin [d], Kiichiro Nakajima [e], Yuki Hirota [f], Shinji Kawabata [f], Tei-ichi Nishiki [a], Iori Ohmori [a], Kazuhito Tomizawa [g], Shin-ichi Miyatake [f], Koji Ono [b], Hideki Matsui [a]

[a] Department of Physiology, Okayama University Graduate School of Medicine, Dentistry and Pharmaceutical Sciences, 2-5-1 Shikata-cho, Kita-Ku, Okayama City, Okayama 700-8558, Japan
[b] Particle Radiation Oncology Research Center, Research Reactor Institute, Kyoto University, Kumatori-cho, Osaka 590-0494, Japan
[c] Department of Applied Chemistry, Faculty of Science and Engineering, Kinki University, 3-4-1 Kowakae, Higashi-Osaka City, Osaka 577-8502, Japan
[d] Department of Biotechnology, Dalian Medical University, No. 9 West Section, Lvshun South, Dalian 116044, China
[e] KNC Laboratories, Ltd., 1-1-1, Murotani, Nishi-ku, Kobe City, Hyogo 651-2241, Japan
[f] Department of Neurosurgery, Osaka Medical College, 2-7 Daigaku-machi, Takatsuki City, Osaka 569-8686, Japan
[g] Department of Molecular Physiology, Faculty of Life Sciences, Kumamoto University, 1-1-1 Honjou, Kumamoto City, Kumamoto 860-8556, Japan

ARTICLE INFO

Article history:
Received 4 December 2013
Accepted 19 December 2013
Available online 20 January 2014

Keywords:
Protein transduction
BSH poly-arginine
TAT
Oron neutron capture therapy (BNCT)

ABSTRACT

New anti-cancer therapy with boron neutron capture therapy (BNCT) is based on the nuclear reaction of boron-10 with neutron irradiation. The median survival of BNCT patients with glioblastoma was almost twice as long as those receiving standard therapy in a Japanese BNCT clinical trial. In this clinical trial, two boron compounds, BPA (boronophenylalanine) and BSH (sodium borocaptate), were used for BNCT. BPA is taken up into cells through amino acid transporters that are expressed highly in almost all malignant cells, but BSH cannot pass through the cell membrane and remains outside the cell. We simulated the energy transfer against the nucleus at different locations of boron from outside the cell to the nuclear region with neutron irradiation and concluded that there was a marked difference between inside and outside the cell in boron localization. To overcome this disadvantage of BSH in BNCT, we used a cell-penetrating peptide system for transduction of BSH. CPP (cell-membrane penetrating peptide) is very common peptide domains that transduce many physiologically active substances into cells *in vitro* and *in vivo*. BSH-fused CPPs can penetrate the cell membrane and localize inside a cell. To increase the boron ratio in one BSH-peptide molecule, 8BSH fused to 11R with a dendritic lysine structure was synthesized and administrated to malignant glioma cells and a brain tumor mouse model. 8BSH-11R localized at the cell nucleus and showed a very high boron value in ICP results. With neutron irradiation, the 8BSH-11R administrated group showed a significant cancer killing effect compared to the 100 times higher concentration of BSH-administrated group. We concluded that BSH-fused CPPs were one of the most improved and potential boron compounds in the next-stage BNCT trial and 8BSH-11R may be applied in the clinical setting.

1. Introduction

For decades, malignant glioma, especially glioblastoma (GBM) was not curable, but in 2004, a randomized phase III trial by the European Organization for the Research and Treatment of Cancer (EORTC) and the National Cancer Institute of Canada Clinical Trials Group (NCIC) reported improved median and 2-year survival of patients with glioblastoma treated with concomitant and adjuvant temozolomide (TMZ) and radiotherapy [1]. The median survival was 14.6 months with radiotherapy plus TMZ and 12.1 months with radiotherapy alone. Furthermore, recently, the Japanese boron neutron capture therapy (BNCT) group against malignant brain tumor reported that the median survival of newly-diagnosed glioblastoma patients with BNCT was 23.5 months [2]. This BNCT outcome is excellent and hopeful for malignant glioma patients.

* Corresponding author. Tel.: +81 86 235 7105; fax: +81 86 235 7111.
E-mail address: hmichiue@md.okayama-u.ac.jp (H. Michiue).

0142-9612/$ – see front matter © 2013 Elsevier Ltd. All rights reserved.
http://dx.doi.org/10.1016/j.biomaterials.2013.12.055

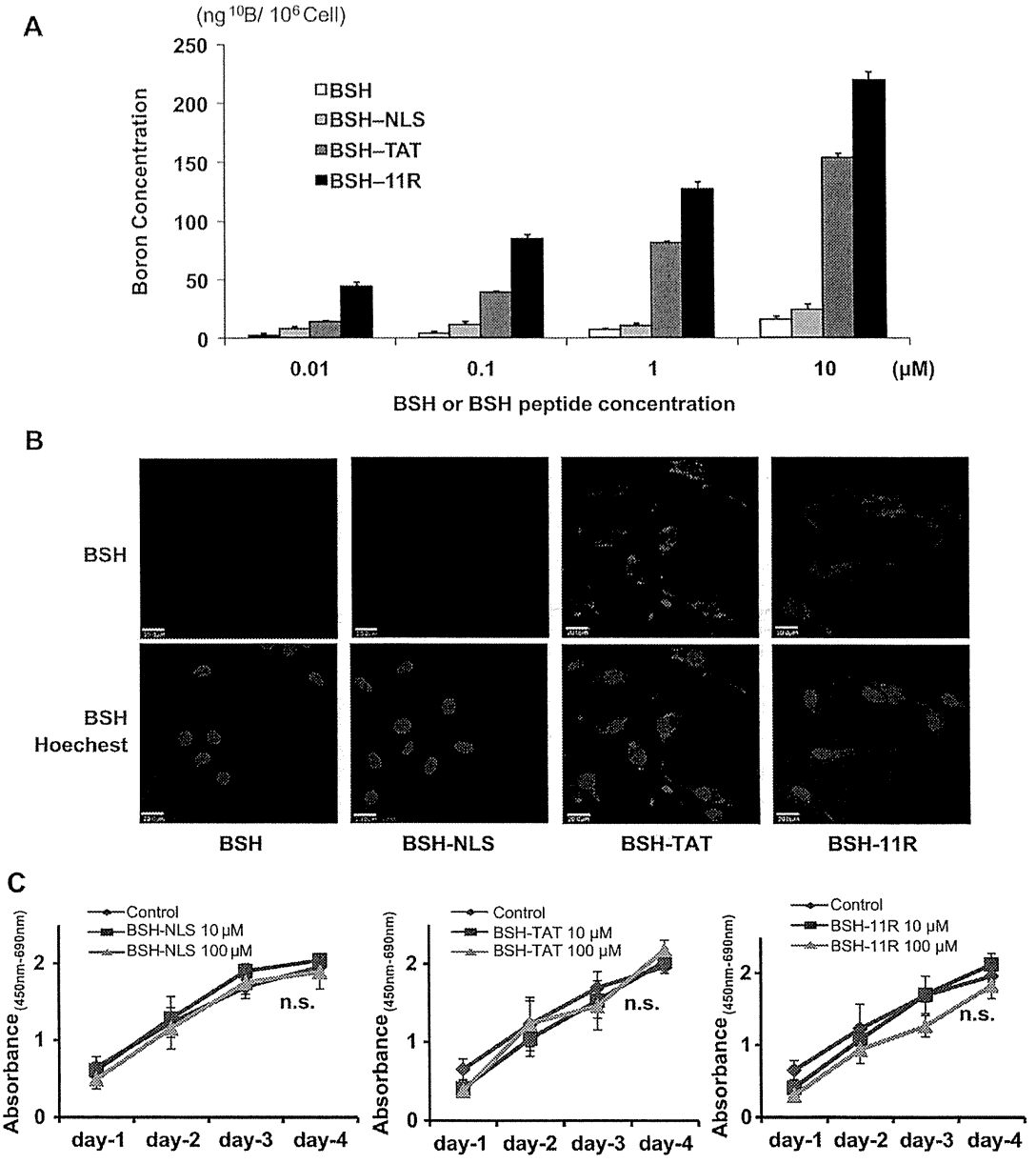

Fig. 1. Administration of BSH-peptide into U87 delta EGFR cell and evaluation of intra-cellular function 1-A: Boron concentration of U87 delta EGFR cells administrated different kinds of BSH and BSH-peptide at 0.01, 0.1, 1 and 10 μM for 12 h. 1-B: Immunocytochemistry showing BSH (red) and nucleus (blue) with identified BSH antbody and Hoechst 33342 by confocal microscopy. Scale bar = 20 μm 1-C: Three graphs showing cell proliferation after administration of each BSH or BSH-peptide at 10 or 100 μM for 4 days by the measurement of absorbance (450 nm-690 nm) with WST-1 reagent. (For interpretation of the references to colour in this figure legend, the reader is referred to the web version of this article.)

BNCT is based on the nuclear capture and fission reactions that occur when boron-10, a non-radioactive isotope and a constituent of natural elemental boron, is irradiated with low energy (<0.025 eV) thermal neutrons (*n*th) to produce high energy (2.3 MeV) alpha (α) particles and recoiling lithium-7 nuclei ($^{10}B + nth \rightarrow [^{11}B] \rightarrow {}^4He(\alpha) + {}^7Li + 2.38$ MeV) [3,4]. BNCT has been used to treat patients with high-grade primary brain tumors and a much smaller number of patients with other types of brain tumors [2,5,6]. For BNCT to be successful, there must be high uptake of ^{10}B by the tumor and low levels in the normal brain, and sufficient fluence of thermal neutrons must be delivered to the tumor. In their BNCT, two low molecular weight ^{10}B-containing drugs, boronophenylalanine (BPA) and/or sodium borocaptate (BSH), were used as capture agents [7]. Two boron compounds have been used clinically: sodium undecahydro-mercaptocloso-dodecaborate ($Na_2B_{12}H_{11}SH$, also referred to as sodium borocaptate or 'BSH') in Japan and Europe and 4-dihydroxyborylphenylalanine (boronophenylalanine or 'BPA') in the United States [4,8]. BPA can enter and accumulate in malignant cells, but BSH shows leakage from the tumor area and cannot transduce into cells [4]. The nuclear reaction caused by BNCT outside cells is mildly effective against malignant cells, but a precise simulation dependent on the intracellular